
ADAPTIVE SMOOTH ACTIVATION FOR IMPROVED DISEASE DIAGNOSIS AND ORGAN SEGMENTATION FROM RADIOLOGY SCANS

A PREPRINT

Koushik Biswas, Debesh Jha, Nikhil Kumar Tomar, Gorkem Durak, Alpay Medetalibeyoglu, Matthew Antalek, Yury Velichko, Daniela Ladner, Amir Bohrani, Ulas Bagci

Machine & Hybrid Intelligence Lab, Department of Radiology, Northwestern University

ABSTRACT

In this study, we propose a new activation function, called Adaptive Smooth Activation Unit (ASAU), tailored for optimized gradient propagation, thereby enhancing the proficiency of convolutional networks in medical image analysis. We apply this new activation function to two important and commonly used general tasks in medical image analysis: automatic disease diagnosis and organ segmentation in CT and MRI. Our rigorous evaluation on the RadImageNet abdominal/pelvis (CT and MRI) dataset and Liver Tumor Segmentation Benchmark (LiTS) 2017 demonstrates that our ASAU-integrated frameworks not only achieve a substantial (4.80%) improvement over ReLU in classification accuracy (disease detection) on abdominal CT and MRI but also achieves 1%-3% improvement in dice coefficient compared to widely used activations for ‘healthy liver tissue’ segmentation. These improvements offer new baselines for developing a diagnostic tool, particularly for complex, challenging pathologies. The superior performance and adaptability of ASAU highlight its potential for integration into a wide range of image classification and segmentation tasks.

Keywords Deep Learning · Medical Imaging · Segmentation · Activation Function

1 Introduction

Computer Aided Detection (Classification): Detecting pathologies from CT and MRI scans automatically is crucial for accurate diagnosis, early detection, and treatment planning. Abdominal CT exams are cost-effective and widely available, making them essential for emergency conditions and detecting lesions. They provide quick and high-resolution images that are particularly useful for identifying acute abdominal pathologies and abdominal tumors. On the other hand, abdominal MRI images provide superior soft tissue contrast and are more effective in classifying tumor types without using ionizing radiation. Automated disease detection from abdominal scans (CT, MRI) plays a pivotal role in the rapid and accurate diagnosis of critical emergencies such as acute pancreatitis, acute appendicitis, and various tumoral lesions affecting organs such as the pancreas, liver, and kidneys. Missed diagnoses of conditions like acute pancreatitis can be life-threatening, which highlights the critical role of automated detection systems in preventing potential mortalities.

Early detection is particularly important for conditions like precursor pancreatic lesions, where timely identification can significantly impact prognosis and patient outcomes. The potential occurrence of pancreatic cancer underlines the importance of rapid intervention at an earlier stage, given the poor prognosis associated with delayed detection. The automatic detection and classification of liver lesions as benign or malignant is crucial for follow-up procedures and treatment strategies. Similarly, detecting lesions in organs like the prostate and adrenal glands helps in patient management and prognosis. Accurately interpreting abdominal scans for these conditions is essential for guiding healthcare professionals in making informed decisions about treatment approaches and ensuring optimal patient care. After all, automated disease detection in abdominal imaging not only improves diagnostic accuracy but also has the potential to significantly enhance prognosis, patient management, and the quality of healthcare services.

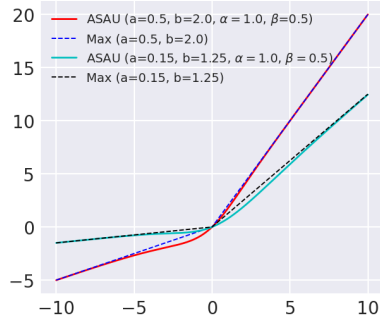


Figure 1: Approximation of Maximum function using ASAU for varying values of a , b , α , and β . As $\beta \rightarrow \infty$, ASAU smoothly approximates the maximum function.

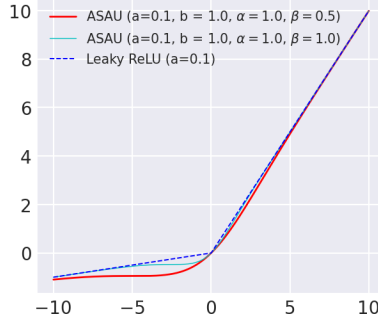


Figure 2: Approximation of Leaky ReLU using ASAU for different values of a , b , α , and β . As $\beta \rightarrow \infty$, ASAU smoothly approximates Leaky ReLU.

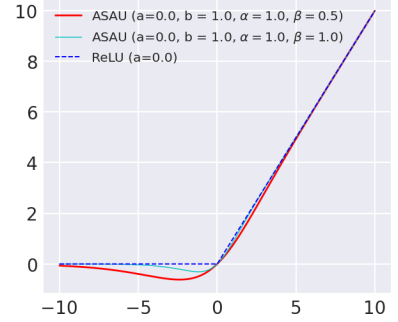


Figure 3: Approximation of ReLU using ASAU for different values of a , b , α , and β . As $\beta \rightarrow \infty$, ASAU smoothly approximates ReLU.

Abdominal anatomy is complex and variable, with numerous organs and structures closely packed together. As a result, distinguishing between healthy and pathological tissues in earlier phases can be challenging due to subtle differences Reyes et al. [2008]. This complexity can lead to variability in interpretation among radiologists, particularly with rare or special conditions. CAD-based algorithms can be helpful in reducing diagnostic errors and improving diagnosis.

Organ Segmentation: For segmentation motivation, we would like to focus on the liver organ for an example, although what we propose herein is generic and can be applied to any organ, pathology, and non-medical applications. We choose the liver because liver cancer is the third most common cause of cancer-related death worldwide Arnold et al. [2020], and the liver needs to be quantified either by volume for several diseases, and also its labelled boundary is used for CAD systems where algorithms seek for lesions inside the liver volume. Besides, the liver is one of the most challenging organs to segment because of its highly variable shape and close proximity to other organs. Liver segmentation is a prerequisite also for the localization of tumors for targeted therapies and the detailed planning of surgical interventions. It demands the highest levels of precision, as the outcomes can directly influence therapeutic decisions and patient prognosis. The variability in contrast, shape, and appearance of liver tissue poses significant challenges. Therefore, automated methods can play an essential role in handling such complexity.

Domain specific activation functions are needed: Current deep learning approaches have shown promise in enhancing the quality of classification and segmentation tasks Jha et al. [2020], Tomar et al. [2022], jha [2023]. However, they are often constrained by the limitations of the activation functions utilized, particularly in convolutional neural networks (CNNs). Traditional activation functions such as ReLU Nair and Hinton [2010] and its variant (for example, Leaky ReLU Xu et al. [2015], PReLU He et al. [2015]), despite being instrumental to the success of CNN, exhibit notable shortcomings. They are prone to information loss in areas of negative input and often fail to capture the subtle nuances necessary for delineating intricate anatomical features, leading to potential inaccuracies in segmentations, which are highly undesirable in a clinical setting. This necessitates the development of more specialized functions tailored to the domain-specific needs of medical image analysis.

Our proposal: Here, we present a novel smooth activation function called the Adaptive Smooth Activation Function (ASAU), carefully designed to handle the challenges prevalent in medical image analysis. This function embodies a methodological shift towards smoother, more continuous transitions, offering refined gradients that promote the intricate learning necessary for high-fidelity classification and segmentation tasks. With the rigorous testing and empirical evaluation on classification and segmentation tasks, our research indicates that applying this ASAU within conventional CNN architectures can substantially enhance the classification for multiclass disease detection from abdominal scans and liver segmentation from CT scans. Our main contributions are:

- We have introduced a novel Adaptive Smooth Activation Function (ASAU) that significantly enhances the classification (disease detection) and segmentation (liver) accuracy.
- Our extensive comparative analysis using Abdomen/Pelvis benchmark classification and healthy liver segmentation datasets in both CT and MRI modalities demonstrates almost 5% improvement in accuracy in both CT and MRI cases and 1% improvement for segmentation tasks (for an organ such as liver, 1% is a significant increment) that show the effectiveness of ASAU.

Table 1: Activation functions and their impact on RadImageNet 28 classes Abdominal/Pelvis CT Scans.

Activation Function	Method	Macro Average			Micro Average			Accuracy	MCC
		Precision	Recall	F1-score	Precision	Recall	F1-score		
ReLU	ResNet-50	35.74	23.16	23.35	67.67	67.67	67.67	67.67	52.84
LReLU	ResNet-50	35.97	23.56	23.65	68.10	68.10	68.10	68.10	53.37
PReLU	ResNet-50	36.30	23.89	23.77	68.77	68.77	68.77	68.77	54.10
ASAU	ResNet-50	46.29	31.30	34.15	72.47	72.47	72.47	72.47	61.10
ReLU	ResNet-18	33.70	25.83	27.43	70.12	70.12	70.12	70.12	57.10
Leaky ReLU	ResNet-18	33.91	25.98	27.60	70.38	70.38	70.38	70.38	57.52
PReLU	ResNet-18	34.20	26.31	27.99	70.52	70.52	70.52	70.52	57.67
ASAU	ResNet-18	36.50	27.30	28.99	71.10	71.10	71.10	71.10	58.59

Table 2: Activation functions and their impact across 26 Classes in RedImageNet Abdominal/Pelvis MRI Scans.

Activation Function	Method	Macro Average			Micro Average			Accuracy	MCC
		Precision	Recall	F1-score	Precision	Recall	F1-score		
ReLU	ResNet-50	40.43	24.83	28.04	86.86	86.86	86.86	86.86	62.92
LReLU	ResNet-50	40.56	24.99	28.56	87.10	87.10	87.10	87.10	63.25
PReLU	ResNet-50	41.10	25.20	28.81	87.25	87.25	87.25	87.25	63.47
ASAU	ResNet-50	44.46	33.23	36.17	89.20	89.20	89.20	89.20	69.75
ReLU	ResNet-18	35.15	26.66	28.82	87.96	87.96	87.96	87.96	66.65
LReLU	ResNet-18	35.67	26.87	28.99	88.12	88.12	88.12	88.12	66.72
PReLU	ResNet-18	35.91	26.80	29.10	88.27	88.27	88.27	88.27	66.81
ASAU	ResNet-18	38.58	27.58	29.67	88.62	88.62	88.62	88.62	67.32

2 Method

2.1 Adaptive Smooth Activation Function

We present the Adaptive Smoothing Activation Unit (ASAU) as a way of learning to activate the neurons or not. In this paper, we show how to approximate the maximum function using a smooth function. We consider the maximum function of two values, $\max(x_1, x_2)$, which is defined as follows:

$$\max(x_1, x_2) = \begin{cases} x_1, & \text{if } x_1 \geq x_2 \\ x_2, & \text{otherwise} \end{cases} \quad (1)$$

We can rewrite the equation (1) as follows:

$$\max(x_1, x_2) = x_1 + \max(0, x_2 - x_1). \quad (2)$$

Note that the maximum function is not differentiable at the origin, but we need differentiable functions during backpropagation. Also, note that the popular activation functions like ReLU Nair and Hinton [2010], Leaky ReLU Maas et al. [2013], and Parametric ReLU are special cases of the maximum function, and they are not differentiable at the origin. Mish Misra [2020] is a smooth activation function that is handcrafted and fixed. If we can add a parameter β in Mish, it can approximate the ReLU activation function smoothly. Note that,

$$\text{if } \beta \rightarrow \infty, \text{ then } x \tanh(\alpha \text{SoftPlus}(\beta x)) \approx \max(0, x) \quad (3)$$

where α is another smoothing parameter and SoftPlus is defined as $\ln(1 + e^x)$. Maxout activation Goodfellow et al. [2013] is a linear combination of the convex functions that generalize the ReLU or its variants. Replacing the equation (3) in equation (2), we have

$$\max(x_1, x_2) \approx x_1 + (x_2 - x_1) \tanh(\alpha \text{SoftPlus}(\beta(x_2 - x_1))) \quad (4)$$

If we consider $x_1 = ax$ and $x_2 = bx$ we can get an approximation of the Maxout family; in particular, we can derive the smooth approximation of the Leaky ReLU and ReLU activation function (by considering $a = 1$ or $a = 0$ respectively).

$$\max(ax, bx) \approx ax + (b - a)x \tanh(\alpha \text{SoftPlus}(\beta(b - a)x)) \quad (5)$$

Figure (1) shows how the maxout has been approximated with the ASAU function. Similarly, Figure (2) and Figure (3) show how the Leaky ReLU and ReLU are approximated with the ASAU function, respectively.

3 Experiments

3.1 Datasets

For the classification tasks, we use RadImageNet Mei et al. [2022] database, which is an open-access medical imaging database designed to improve transfer learning performance on downstream medical imaging applications and perhaps

Table 3: Comparison of different activation functions on liver segmentation benchmark (LiTS) dataset.

Activation Function	UNet Ronneberger et al. [2015]				DoubleUNet Jha et al. [2020]				ColonSegNet Jha et al. [2021a]				UNext Valanarasu and Patel [2022]			
	mDSC	mIoU	Rec.	Prec.	mDSC	mIoU	Rec.	Prec.	mDSC	mIoU	Rec.	Prec.	mDSC	mIoU	Rec.	Prec.
ReLU	82.06	73.40	77.82	91.10	86.24	77.89	80.68	95.00	80.87	71.71	80.07	87.50	80.27	71.31	78.84	87.82
LReLU	82.47	73.98	78.46	91.17	86.27	78.21	80.20	95.67	80.84	71.69	79.31	88.10	80.92	72.15	76.84	90.85
PReLU	82.71	73.91	78.77	91.21	86.39	78.09	80.39	95.59	78.91	69.85	77.89	86.27	79.08	69.95	77.38	88.55
ASAU	83.62	75.08	80.59	93.29	86.88	78.73	80.77	96.58	83.03	74.18	78.79	91.17	81.98	73.03	79.01	90.45

Table 4: Comparison of different activation functions on liver tumor segmentation benchmark (LiTS) Benchmark dataset.

Activation Function	TransNetR Jha [2023]				TransResUNet Tomar et al. [2022]				ResUNet++ Jha et al. [2019]				NanoNet-A Jha et al. [2021b]			
	mDSC	mIoU	Rec.	Prec.	mDSC	mIoU	Rec.	Prec.	mDSC	mIoU	Rec.	Prec.	mDSC	mIoU	Rec.	Prec.
ReLU	86.11	77.95	80.16	96.34	86.38	78.23	80.85	95.77	77.03	68.19	79.90	83.57	75.05	66.53	73.33	83.25
LReLU	86.30	78.37	80.37	96.67	86.18	77.82	79.80	96.59	75.03	66.35	71.64	84.05	74.05	65.02	73.36	84.23
PReLU	86.39	78.29	80.32	96.52	85.68	77.30	79.46	96.12	74.39	66.02	74.38	81.99	74.84	66.08	72.47	85.24
ASAU	86.41	78.49	80.30	96.65	86.35	78.15	79.89	96.67	78.12	69.56	81.50	83.81	76.57	67.30	75.88	84.61

the largest ever medical imaging dataset so far. From the whole dataset, we experiment on CT abdominal/pelvis, consisting of 28 disease classes with an average class size of 4994 and a total of 139,825 slices (i.e., the dataset is designed to have slices per disease although the scans are volumes-3D). The CT dataset contains 28 (disease) classes such as adrenal pathology, arterial pathology, ascites, bil dil, bladder pathology, bowel abnormality, bowel inflammation, bowel mass degenerative changes, dilated urinary tract, fat-containing tumor, gallbladder pathology, gallstone, intraperitoneal mass, liver lesion, normal osseous, neoplasm, ovarian pathology, pancreatic lesion, post-op, prostate lesion, renal lesion, soft tissue collection, soft tissue mass, splenic lesion, urolithiasis and uterine pathology. We also experimented on the MRI abdomen/pelvis dataset consisting of 26 distinct (disease) classes with an average class size of 3513 slices and a total number of 91,348 slices. While most of these classes overlap with the CT dataset, the MRI dataset uniquely includes classes like enlarged organs and liver disease, which are not in the CT dataset. The CT dataset, conversely, has a specific class for entire abdominal organs.

For the segmentation tasks, we select the Liver Tumor Segmentation Benchmark (LiTS) Bilic et al. [2023] dataset, which is a multi-center dataset collected from seven clinical centers. It contains 201 CT images of the abdomen. The dataset is completely anonymized, and the images have been reviewed visually to preclude the presence of personal identifiers. The whole dataset is distributed into a training dataset with 130 CT scans, and the test dataset has 71 CT scans. Only the training dataset is made publically available. Thus, we trained the dataset for our experimentation.

3.2 Implementation details

We used the PyTorch Paszke et al. [2019] framework for all the segmentation experiments. The networks were configured to train for liver segmentation tasks with a batch size of 16 and a learning rate set to $1e^{-4}$. 500 epochs of training were performed to fine-tune the network parameters adequately with an early stopping patience of 50. To enhance the performance of our network, we used a combination of binary cross-entropy and dice loss, and an Adam optimizer was chosen for parameter updates. The data was split into 80% for training, 10% for validation, and 10% for testing. We resized the image to 256×256 pixels in-plane resolution to optimize the trade-off between training time and model complexity. To avoid bias, we also split the cases into independent training (70 patients), validation (30 patients), and test (30 patients) sets. The volumetric CT scans were processed pseudo-3D (slice-by-slice) to fit into regular computer hardware (GPU). During preprocessing, we extracted the healthy liver masks.

For classification (disease detection) experiments, we consider Tensorflow-Keras Chollet et al. [2015] framework. We consider ResNet-18 He et al. [2016a] and ResNet-50 He et al. [2016a] as our baseline classification networks. The networks are trained with batch size 32, initial learning rate 0.00001 with Adam Kingma and Ba [2017] optimizer and $1e^{-4}$ weight decay rate. The data was split into 80% for training, 10% for validation, and 10% for testing. Results are reported on CT scan image data in Table 1 and MRI image data in Table 2.

3.3 Results and Discussion

Table 1 shows the results of ResNet-50 He et al. [2016b] and ResNet-18 architectures on the CT abdominal/pelvis scan dataset. Here, we examine the efficacy of ReLU, LReLU, and PReLU activation along with our proposed ASAU. For all the experiments, the ASAU-based method outperformed all other experimental settings in all the metrics with a significant margin. On the ResNet-50-based architecture, the ASAU integrated method obtains a high improvement of 8.26% in terms of MCC. Table 2 shows the MRI abdominal/pelvis dataset results. Again, here, ASU-integrated ResNet50 obtained an MCC score of 69.75%, which is 6.83% better than ReLU based method.

Table 3 and Table 4 show LiTs datasets’ results. Here, we have compared the performance of eight state-of-the-art medical image segmentation methods (UNet Ronneberger et al. [2015], DoubleUNet Jha et al. [2020], ColonSegNet Jha et al. [2021a], UNext Valanarasu and Patel [2022], TransNetR jha [2023], TransResNet Tomar et al. [2022], ResUNet++ Jha et al. [2019] and NanoNet-A Jha et al. [2021b]) with four different activation functions. From the table, it can be observed that ASAU has significant improvement from 1% to 3% as compared to the ReLU activation function. DoubleUNet, along with ASAU, has set a new baseline for liver segmentation tasks with a high dice score of 86.88%, mIoU of 78.73%, recall of 80.77%, and precision of 96.58%.

4 Conclusion

Our study introduces a pioneering activation function, Adaptive Smooth Maximum Unit (ASAU), to enhance the classification of abdominal organs and segment abdominal liver CT images. The promising results attained by our framework on the RadImageNet and LiTS datasets underscore its potential applicability to a broader range of organ imaging tasks. Future research endeavors are directed towards harnessing three-dimensional spatial information more effectively, aiming to refine the diagnostic tools available to clinicians further and potentially extend the application of our method to include a comprehensive suite of abdominal organs, enhancing our approach’s overall robustness and generalization.

Compliance with Ethical Standards

This research study was conducted retrospectively using human subject data made available in open access by. Ethical approval was not required, as confirmed by the license attached with the open-access data.

Conflicts of Interest

The authors have no relevant financial interests to disclose.

References

- Mauricio Reyes, Miguel A Gonzalez Ballester, Zhixi Li, Nina Kozic, Ronald M Summers, and Marius George Linguraru. Interpretability of anatomical variability analysis of abdominal organs via clusterization of decomposition modes. In *Proceedings of the International Conference of the IEEE Engineering in Medicine and Biology Society*, pages 355–358, 2008.
- Melina Arnold, Christian C Abnet, Rachel E Neale, Jerome Vignat, Edward L Giovannucci, Katherine A McGlynn, and Freddie Bray. Global burden of 5 major types of gastrointestinal cancer. *Gastroenterology*, 159(1):335–349, 2020.
- Debesh Jha, Michael A Riegler, Dag Johansen, Pål Halvorsen, and Håvard D Johansen. DoubleU-Net: A Deep Convolutional Neural Network for Medical Image Segmentation. In *Proceedings of the IEEE 33rd International Symposium on computer-based medical systems (CBMS)*, pages 558–564, 2020.
- Nikhil Kumar Tomar, Annie Shergill, Brandon Rieders, Ulas Bagci, and Debesh Jha. TransResU-Net: Transformer based ResU-Net for real-time colonoscopy polyp segmentation. *arXiv preprint arXiv:2206.08985*, 2022.
- TransNetR: Transformer-based Residual Network for Polyp Segmentation with Multi-Center Out-of-Distribution Testing*, 2023.
- Vinod Nair and Geoffrey E Hinton. Rectified linear units improve restricted boltzmann machines. In *Proceedings of the 27th international conference on machine learning (ICML-10)*, pages 807–814, 2010.
- Bing Xu, Naiyan Wang, Tianqi Chen, and Mu Li. Empirical evaluation of rectified activations in convolutional network. *arXiv preprint:1505.00853*, 2015.
- Kaiming He, Xiangyu Zhang, Shaoqing Ren, and Jian Sun. Delving deep into rectifiers: Surpassing human-level performance on imagenet classification. In *Proceedings of the IEEE international conference on computer vision*, pages 1026–1034, 2015.
- Andrew L Maas, Awni Y Hannun, Andrew Y Ng, et al. Rectifier nonlinearities improve neural network acoustic models. In *Proc. icml*, volume 30, page 3, 2013.
- Diganta Misra. Mish: A self regularized non-monotonic activation function, 2020.
- Ian J. Goodfellow, David Warde-Farley, Mehdi Mirza, Aaron Courville, and Yoshua Bengio. Maxout networks, 2013.
- Olaf Ronneberger, Philipp Fischer, and Thomas Brox. U-Net: Convolutional Networks for Biomedical Image Segmentation. In *Proceedings of the 18th International Conference on Medical Image Computing and Computer-Assisted Intervention*, pages 234–241, 2015.

- Debesh Jha, Sharib Ali, Nikhil Kumar Tomar, Håvard D Johansen, Dag Johansen, Jens Rittscher, Michael A Riegler, and Pål Halvorsen. Real-Time Polyp Detection, Localization and Segmentation in Colonoscopy using Deep Learning. *IEEE Access*, 9:40496–40510, 2021a.
- Jeya Maria Jose Valanarasu and Vishal M. Patel. Unext: Mlp-based rapid medical image segmentation network, 2022.
- Debesh Jha, Pia H Smedsrud, Michael A Riegler, Dag Johansen, Thomas De Lange, Pål Halvorsen, and Håvard D Johansen. ResUNet++: An Advanced Architecture for Medical Image Segmentation. In *Proc. of int. symposium on multimedia*, pages 225–2255, 2019.
- Debesh Jha, Nikhil Kumar Tomar, Sharib Ali, Michael A Riegler, Håvard D Johansen, Dag Johansen, Thomas de Lange, and Pål Halvorsen. Nanonet: Real-time polyp segmentation in video capsule endoscopy and colonoscopy. In *Proceedings of the International Symposium on Computer-Based Medical Systems (CBMS)*, pages 37–43, 2021b.
- Xueyan Mei, Zelong Liu, Philip M Robson, Brett Marinelli, Mingqian Huang, Amish Doshi, Adam Jacobi, Chendi Cao, Katherine E Link, Thomas Yang, et al. RadImageNet: RadImageNet: An Open Radiologic Deep Learning Research Dataset for Effective Transfer Learning. *Radiology: Artificial Intelligence*, 4(5):e210315, 2022.
- Patrick Bilic, Patrick Christ, Hongwei Bran Li, Eugene Vorontsov, Avi Ben-Cohen, Georgios Kaissis, Adi Szeskin, Colin Jacobs, Gabriel Efrain Humpire Mamani, Gabriel Chartrand, et al. The liver tumor segmentation benchmark (lits). *Medical Image Analysis*, 84:102680, 2023.
- Adam Paszke, Sam Gross, Francisco Massa, Adam Lerer, James Bradbury, Gregory Chanan, Trevor Killeen, Zeming Lin, Natalia Gimelshein, Luca Antiga, et al. Pytorch: An imperative style, high-performance deep learning library. *Advances in neural information processing systems*, 32, 2019.
- François Chollet et al. Keras. <https://keras.io>, 2015.
- Kaiming He, Xiangyu Zhang, Shaoqing Ren, and Jian Sun. Deep residual learning for image recognition. In *Proceedings of the IEEE conference on computer vision and pattern recognition*, pages 770–778, 2016a.
- Diederik P. Kingma and Jimmy Ba. Adam: A method for stochastic optimization, 2017.
- Kaiming He, Xiangyu Zhang, Shaoqing Ren, and Jian Sun. Deep residual learning for image recognition. In *Proceedings of the IEEE conference on computer vision and pattern recognition*, pages 770–778, 2016b.